*Available online a*t www.pelagiaresearchlibrary.com

Pelagia Research Library

Advances in Applied Science Research, 2014, 5(5):122-138

ISSN: 0976-8610
CODEN (USA): AASRFC

Effects of chemical reaction and radiation absorption on mixed convective flow in a circular annulus at constant heat and mass flux

K. Ramesh Babu[1], B. Venkateswarlu[1] and P. V. Satyanarayana[2]

[1]*Department of Mathematics, Sree Vidyanikethan Engineering College, Tirupati, A.P, India*
[2]*Department of Mathematics, VIT University, Vellore, T. N., India*

ABSTRACT

In this paper, the effects of chemical reaction, radiation absorption on mixed convective heat and mass transfer, flow of a viscous fluid through a porous medium in a cylindrical region between concentric circular cylinders $r = a$ *and* $r = b$ *in the presence of heat generating sources are dealt appropriately. Hear, the outer cylinder* $r = b$ *is maintained at a constant heat and mass flux. The relation between the temperature is explained in the equation of state and constant heat source in the field region. The governing non-linear partial differential equations can be transformed into a system of ordinary differential equations are them solved by using Gauss-Seidal Iteration method. The effect of variation of governing parameters on the flow heat and mass transfer characteristics are discussed through the graphs and tables.*

Keywords: Chemical reaction, Radiation absorption, mixed convection, Porous medium Circular annulus, Cylinder, heat and mass flux

INTRODUCTION

The increasing cost of energy has led the technologists to examine measures which could considerably reduce the usage of the natural source energy. Thermal insulations continue to find increased use as engineers seek to reduce cost. Heat transfer in porous thermal insulation within vertical cylindrical annuli provides us insight into the mechanism of energy transport and enables engineers to use insulation more efficiently. In particular, design engineers require relationship between heat transfer, geometry and boundary conditions which can be utilized for cost–benefit analysis to determine the amount of insulation that yields the maximum investment. Apart from this, the study of flow and heat transfer in the annular region between the concentric cylinders has its applications in the research related to the disposal of nuclear waste.

Free convection in a vertical porous annulus has been extensively studied by **[1-3]** both theoretically and experimentally. A detailed theoretical study of free convection in a horizontal porous annulus, including possible three dimensional and transient effects and similar studies for fluid filled annuli are available in the literature **[4]**. Convection through annular regions under steady state conditions has also been discussed with the two cylindrical surfaces kept at different temperatures **[5]**. This work has been extended in temperature dependent convection flow **[6-7]** as well as convection flow through horizontal porous channel whose inner surface is maintained at constant temperature, while the circumference is maintained at varying sinusoidal temperature **[8-9]**.

Free convection flow and heat transfer in hydro magnetic case is important in nuclear and space technology **[10-15]**. In particular, convection flow in a vertical annulus region in the presence of radial magnetic field has been investigated by Sastry and Bhadram **[16]**. Nanda and Purushothama **[17]** have analyzed the free convection of a thermal conducting viscous incompressible fluid induced by a traveling thermal wave on the circumference of a long vertical circular cylindrical pipe. Ganapathi and Purushotham **[18]** have studied the unsteady flow induced by a traveling thermal wave imposed on the circumference of a long vertical cylindrical column of a fluid in a saturated porous medium. The analysis is carried out following Whitehead **[19]**. The flow is generated by periodic traveling waves imposed on the outer cylinder and the inner cylinder which is maintained at constant temperature. Some recent investigators dealing with the flows of nano and micropolar fluids are given in the references **[20-21]**.

Chen and Yuh **[22]** have investigated the heat and mass transfer characteristics of natural convection flow along a vertical cylinder under the combined buoyancy effects of thermal and species diffusion. The analysis is restricted to the processes in which the thermo-diffusion effects as well as inter facial velocities from species diffusion are negligible. The surface of the cylinder is either maintained at a uniform temperature and concentration (or) subjected to uniform heat and mass flux. Sivanjaneya Prasad **[23]** has investigated the free convection flow of an incompressible, viscous fluid through a porous medium in the annulus between the porous concentric cylinders under the influence of a radial magnetic field. Antonio **[23]** has investigated the laminar flow, heat transfer in a vertical cylindrical duct by taking in to account both viscous dissipation and the effect of buoyancy. The limiting case of fully developed natural convection in porous annuli is solved analytically for steady and transient cases by **[25-26]**. Philip **[27]** has obtained analytical solution for the annular porous media valid for low modified Reynolds number.

From the scientific point of study, flow arising from temperature and material difference is applied in chemical engineering, geothermal reservoirs, aeronautics and astrophysics. In some applications magnetic forces are present and at other times the flow is further complicated by the presence of radiation absorption, an excellent example of this is in the planetary atmosphere where there is radiation absorption from nearby stars. Recently, Venkateswarlu et al. [28] analyzed the chemical reaction and radiation absorption effects on the flow and heat transfer of a nanofluid in a rotating system. Satya Narayana et al. [29] studied the chemical reaction and Radiation absorption effects on MHD micropolar fluid past a vertical porous plate in a rotating system. MHD visco-elastic fluid flow over a continuously moving vertical surface with chemical reaction was studied by **[30]**.

This paper deals with the convective heat and mass transfer flow of a viscous fluid through a porous medium in an annular region between concentric cylinder $r = a$, and $r = b$ in presence of heat generating sources. The outer cylinder $r = b$ is maintained at constant temperature flux and concentration flux. By using Gauss–Seidel Iteration procedure, the governing equations are solved numerically. The effect of variation of governing parameter on the flow heat and mass transfer characteristics are discussed in detail.

Mathematical Formulation

The steady laminar free convective flow of an incompressible, viscous, electrically conducting fluid is analyzed through a porous medium confined in an annular region between two the vertical co-axial porous circular pipes in the presence of heat generating sources. The cylindrical polar coordinates system $O(r,\theta,z)$ is chosen with the inner and outer cylinders at $r = a$ and $r = b$ respectively. The fluid is subjected to the influence of a radial magnetic field (H_0 / r). Pipes being sufficiently long, all the physical quantities are independent of the axial coordinate z. The fluid is chosen to be of small conductivity so that the Magnetic Reynolds number is much smaller than unity and hence the induced magnetic field is negligible compared to the applied radial field. Also the motion being rotationally symmetric, the Azimuthal velocity V is zero.

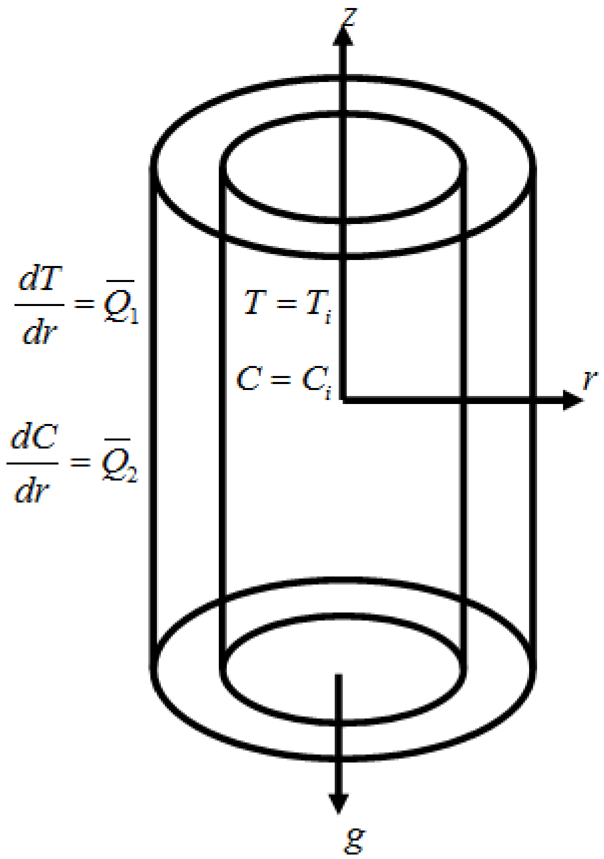

Figure 1: Schematic Diagram of the Configuration

The equation of motion governing the MHD flow through the porous medium are

$$\frac{\partial u}{\partial r} + \frac{u}{r} = 0 \tag{1}$$

$$u\frac{\partial u}{\partial r} = -\frac{1}{\rho_e}\frac{\partial p}{\partial r} + \frac{\mu}{\rho_e}\left\{\frac{\partial^2 u}{\partial r^2} + \frac{1}{r}\frac{\partial u}{\partial r} - \frac{u}{r^2}\right\} - \frac{\mu}{\rho_e k}u \tag{2}$$

$$u\frac{\partial w}{\partial r} = -\frac{1}{\rho_e}\frac{\partial p}{\partial z} + \frac{\mu}{\rho_e}\left\{\frac{\partial^2 w}{\partial r^2} + \frac{1}{r}\frac{\partial w}{\partial r}\right\} - \frac{\mu}{\rho_e k}w - \frac{\rho g}{\rho_e} - \frac{\sigma\mu_e^2 B_0^2}{\rho_e r^2}w \tag{3}$$

$$u\frac{\partial T}{\partial r} = \frac{k_f}{\rho C_p}\left\{\frac{\partial^2 T}{\partial r^2} + \frac{1}{r}\frac{\partial T}{\partial r}\right\} - \frac{Q_H}{\rho C_p}(T - T_e) + \frac{Q_1'}{\rho C_p}(C - C_e) \tag{4}$$

$$u\frac{\partial C}{\partial r} = D\left\{\frac{\partial^2 C}{\partial r^2} + \frac{1}{r}\frac{\partial C}{\partial r}\right\} - k_1 C \tag{5}$$

$$\rho\text{-}\rho_e = -\beta(T - T_0) - \beta^*(C - C_0) \tag{6}$$

The boundary conditions are

$$w=0 \qquad T=T_i \qquad C = C_i \qquad at\ \ r = a$$
$$w = 0 \qquad \frac{dT}{dr} = Q_1 \qquad \frac{dC}{dr} = Q_2 \qquad at\ \ r = b \tag{7}$$

The equation of continuity gives

$$ru = a\frac{\partial u}{\partial a} = b\frac{\partial u}{\partial b} \qquad \frac{\partial u}{\partial b} = \frac{a}{b}\frac{\partial u}{\partial a} \tag{8}$$

In the hydrostatic state equation (3) gives

$$-\rho_e g - -\rho_e z = 0 \tag{9}$$

The pressure in the static case

$$-\rho_e g - \rho_z = -(\rho - \rho_e) g - \rho_{d,z} \tag{10}$$

Substituting equation (10) in equation (2), we find

$$\frac{\partial \mathrm{p_d}}{\partial \mathrm{r}} = \mathrm{f\ (r)} \tag{11}$$

Using the equations (8)–(11) substituting in the equations (1)–(4), the governing free convective heat transfer flows under no pressure gradient are

$$\mathrm{w_{rr}} + \left\{1 - a\frac{u_a}{\nu}\right\}\frac{w_r}{r} + \frac{g\beta}{\nu}(T - T_e) + \frac{g\beta^*}{\nu}(C - C_e) - \frac{\sigma\mu_e^2 H_0^2 a^2}{\nu}\frac{w}{r^2} - \frac{\nu}{k}w = 0 \tag{12}$$

$$\frac{\partial^2 T}{\partial r^2} + \frac{1}{r}\left(1 - \frac{a}{\nu}\frac{\partial u}{\partial a}\right)\frac{\partial T}{\partial r} - \frac{Q_H}{k_f}(T - T_e) + \frac{Q_l'}{k_f}(C - C_e) = 0 \tag{13}$$

$$\frac{\partial^2 C}{\partial r^2} + \frac{1}{r}\left(1 - \frac{a}{\nu}\frac{\partial u}{\partial a}\right)\frac{\partial C}{\partial r} - k_l C = 0 \tag{14}$$

Introducing the non-dimensional variables $(\mathrm{r}', \mathrm{w}', \theta')$ as

$$\begin{array}{lllll} r' = \dfrac{r}{a} & w' = \dfrac{wa}{\nu} & S = \dfrac{a\,u_a}{\nu} & D_2^{-1} = \dfrac{a^2}{k} & Kr = \dfrac{k_1 a^2}{D_1} \\ Q = \dfrac{Q_H L^2}{k_f} & \Pr = \dfrac{\mu C_p}{k_f} & R = \dfrac{\beta^* k_{11}}{\beta\nu} & Sc = \dfrac{\nu}{D_1} & Q_1 = \dfrac{Q_1' \Delta C a^2}{k_f \Delta T} \\ \theta = \dfrac{T - T_e}{T_i - T_e} & C' = \dfrac{C - C_e}{C_i - C_e} & M = \sqrt{\dfrac{\sigma\mu_e^2 H_0^2 a^2}{\rho\nu}} & Gr = \dfrac{\beta g a^3 (T_1 - T_e)^2}{\nu^2} & \end{array} \tag{15}$$

The equations (13) and (14) are reduced to

$$\mathrm{w_{rr}} + \frac{(1-S)}{r}w_r - \left\{D_2^{-1} + \frac{M^2}{r^2}\right\}w = -Gr\{\theta + NC\} \tag{16}$$

$$\frac{\partial^2 \theta}{\partial r^2} + \frac{1}{r}(1 - S\Pr)\frac{\partial \theta}{\partial r} - Q\theta + Q_1 C = 0 \tag{17}$$

$$\frac{\partial^2 C}{\partial r^2} + \frac{1}{r}(1 - SSc)\frac{\partial \theta}{\partial r} - KrC = 0 \tag{18}$$

The corresponding boundary conditions are

$$\begin{array}{lll} w = 0 & \theta = 1 & C = 1 \quad on \quad r = 1 \\ w(s) = 0 & \left(\dfrac{d\theta}{dr}\right)_{r=s} = Q_1 & \left(\dfrac{dC}{dr}\right)_{r=s} = Q_2 \end{array} \tag{19}$$

The method of solution to the problem

The differential equations (16)-(18) have been discussed numerically by reducing the differential equations to difference equations which are solved by using Gauss-Seidel Iteration method. The differential equations involving $\theta_0,\ \theta_1,\ w_0\ and\ w_1$ are reduced to the following difference equations

$$\{1 - h(1 - S\Pr)/2r_i\}\theta_{i-1} - (2+\alpha)\theta_i + \{1 + h(1 - S\Pr)/2r_i\}\theta_{i+1} + Q_1 C_i = 0 \tag{20}$$

$$\{1-h(1-SSc)/2r_i\}C_{i-1}-2C_i+\{1+h(1-SSc)/2r_i\}C_{i+1}-Kr\,C_i=0) \tag{21}$$

$$\left\{1-\frac{h(1-S)}{2r_i}\right\}w_{i-1}-\left\{2+h^2(D_2^{-1}+\frac{M^2}{r^2})\right\}w_i+\left\{1+\frac{h(1-S)}{2r_i}\right\}_i w_{i+1}=-Grh^2(\theta_i+NC_i) \tag{22}$$

The step length h is taken to be 0.05 together with the following conditions

$$\theta_0=1 \quad \theta_{17}=m_1 \quad w_0=0 \quad w_{17}=0$$

All the above difference equations are solved using Gauss-Seidel iterative method to the fourth decimal accuracy. The shear stress on the pipe is given by

$$\tau'=\mu(\frac{\partial w}{\partial r})_{r=a,b}$$

which in the non-dimensional form reduces to $\tau=\tau'/(\mu^2/a^2)=(w_r)_{r=1,s}=(w_{0,r}+E_e w_{1,r})_{r=1,s}$ (23)

The heat transfer through the pipe to the flow per unit area of the pipe surface is given by

$$q=k_1(\frac{\partial T}{\partial r})_{r=a}$$

which in the non-dimensional form is

$$Nu=(\frac{qa}{k_1(T_1-T_e)})=(\frac{\partial\theta}{\partial r})_{r=1} \tag{24}$$

The mass transfer through the pipe to the flow per unit area of the pipe surface in the non-dimensional form is

$$Sh=(\frac{q_1 a}{D_1(C_1-C_e)})=(\frac{\partial C}{\partial r})_{r=1} \tag{25}$$

RESULTS AND DISCUSSION

The object of the present analysis is to study the effects of chemical reaction and radiation absorption on mixed convective flow in a circular annulus at a constant heat and mass flux. The results reported in the previous section preformed and a representative set of results are reported graphically in **figures 2-7.** These results are obtained to illustrate the influence of various parameters on the velocity, temperature and concentration profiles. In order to verify the validity and accuracy of the present analysis, it is compared with the skin friction coefficient, Nusselt number and Sherhwood number. The results of this comparison are given in tables. It is noticed that the comparison shows good agreement and therefore the present results are very accurate. It can be seen from this table that there exists a perfect agreement between the results.

Figure 2(a)-2(c) represents the velocity, temperature and concentration distributions for various values of Grashof number Gr. It is found that the velocity $w>0$ occurs for $Gr<0$ and the velocity $w<0$ occurs for $Gr>0$. This shows that w exhibits a reversal flow for $Gr<0$ and the region of reversal flow enlarges with $|Gr|$. Also the velocity $|w|$ enhancement with increase in $|Gr|$ at $r=1.4$. **Figures 2(b) and 2(c)** represents θ and C with Grashof number Gr, fixing the other parameters. It is observed that the actual temperature and concentration depreciates with $Gr>0$ and enhances with $Gr<0$ with maximum at $r=1$.

For various values of chemical reaction parameter Kr on velocity, temperature and concentration profiles across the boundary layer are shown in **figures 3(a)-3(c).** It is clear from the **figures** that the velocity, temperature and concentration depreciate in the degeneration reaction and enhances in the generating reaction. Further, this **figure** shows that the variation of chemical reaction parameter Kr with temperature increasing tendency, increases in Kr everywhere in the flow region.

Figures 4(a)-4(c) respectively shows the effect of D^{-1} and M on the velocity, temperature and concentration profiles for a stationary porous plate. It is clear that **figure 4(a),** shows the variation of velocity with D^{-1} and M shows that lesser the permeability of the porous medium or higher the Lorentz force smaller $|w|$ in the flow region.

From **figures 4(b) and 4(c),** it is found that the actual temperature and concentration fields enhances with $D^{-1} \le 2\times10^{2}$ and depreciates with higher $D^{-1} \ge 3\times10^{2}$. Higher the Lorentz forces, smaller the actual temperature in the entire flow region.

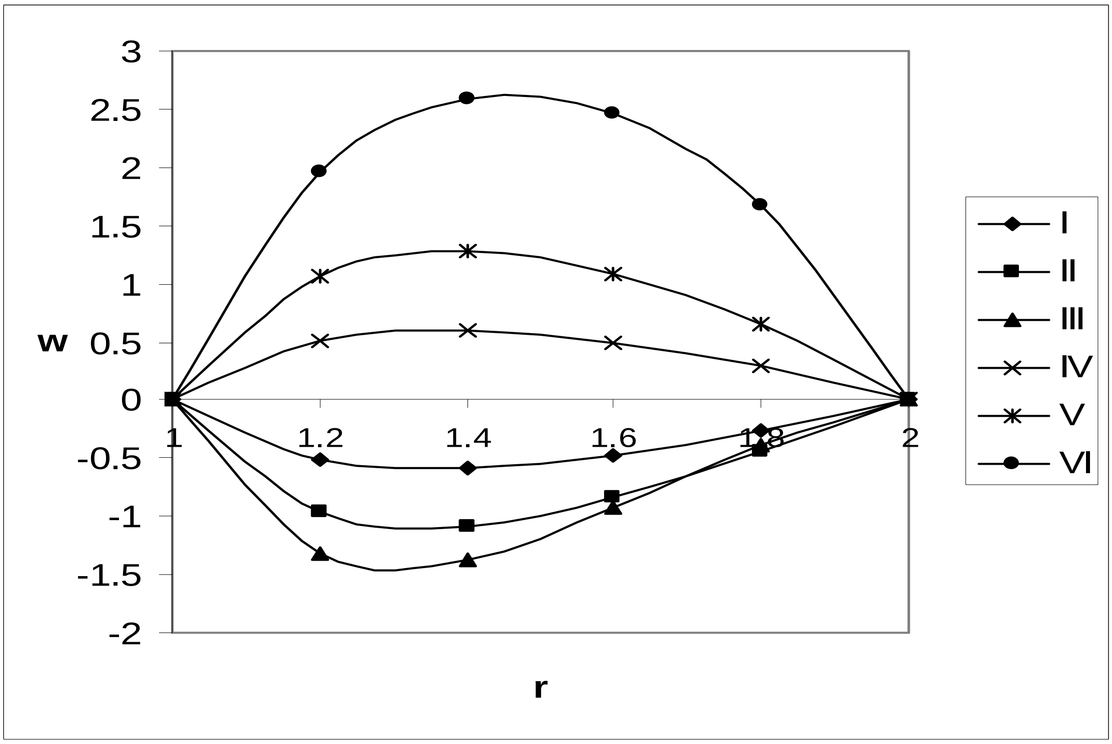

Figure 2(a): Velocity profiles for Variation of Gr

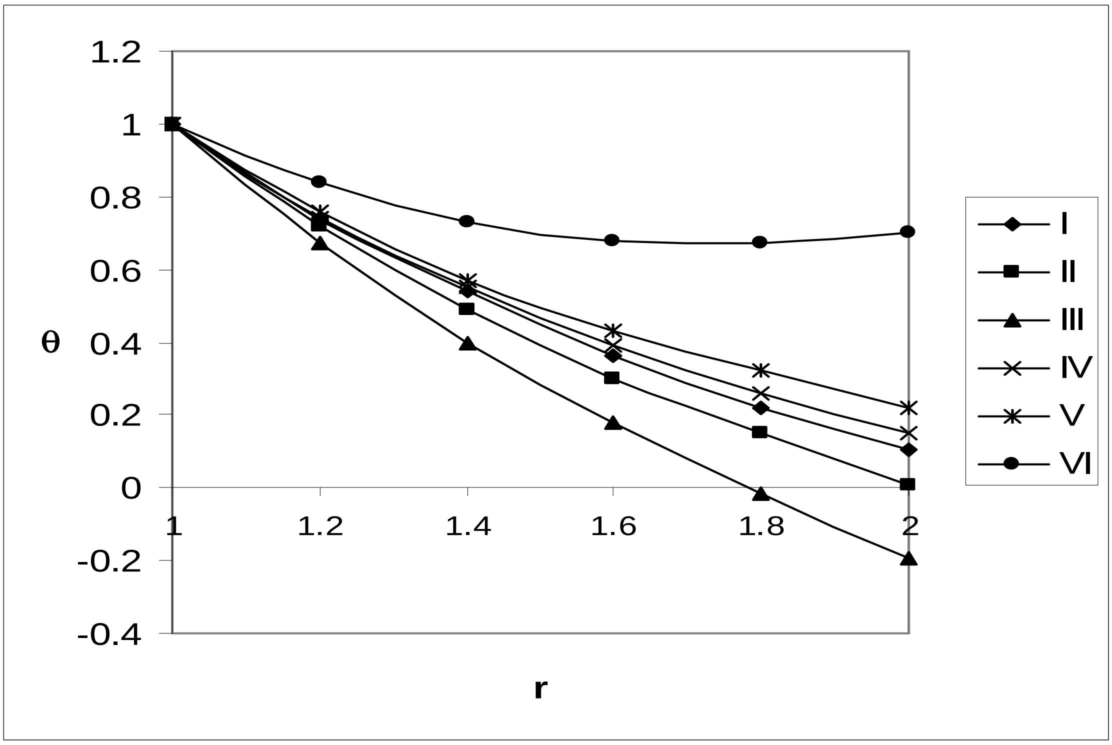

Figure 2(b): Temperature profiles for various values of Gr

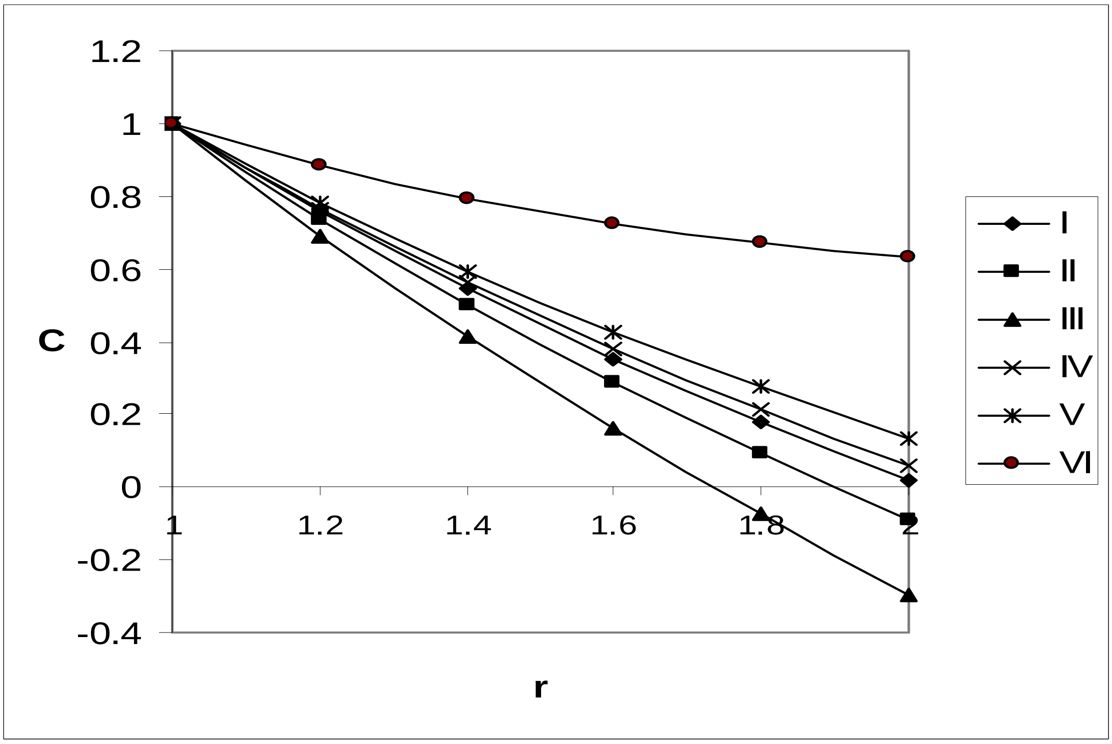

Figure 2(c): Concentration profiles for various values of Gr

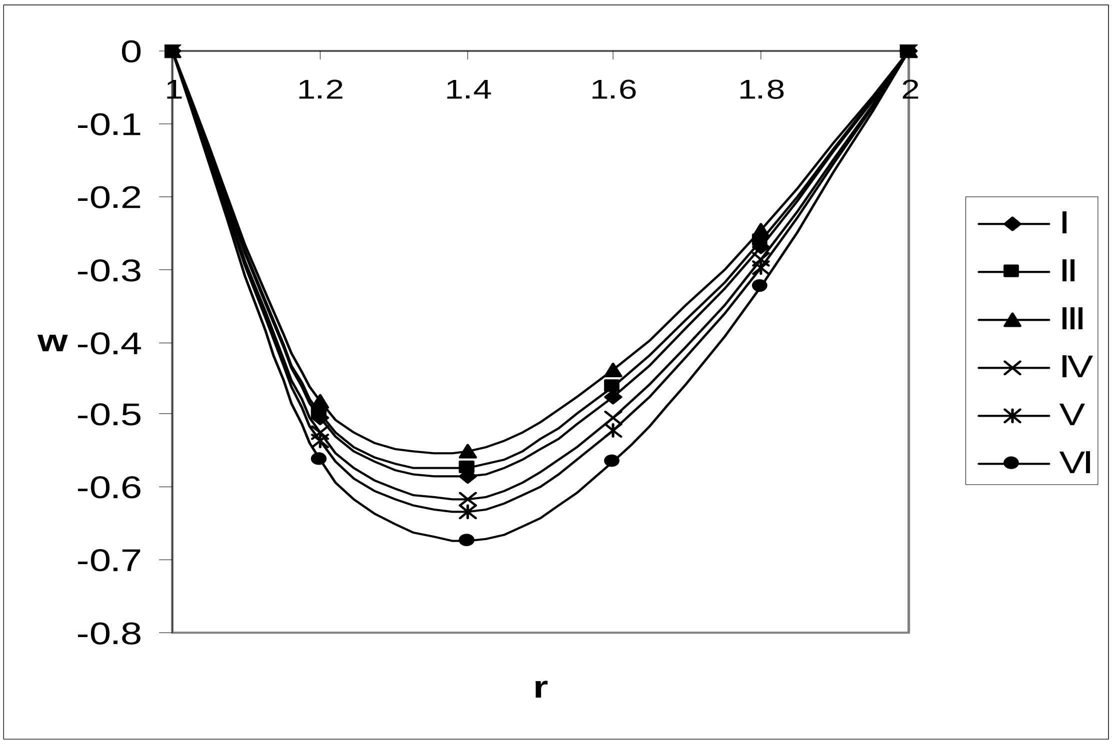

Figure 3(a): Velocity profiles for various values of Kr

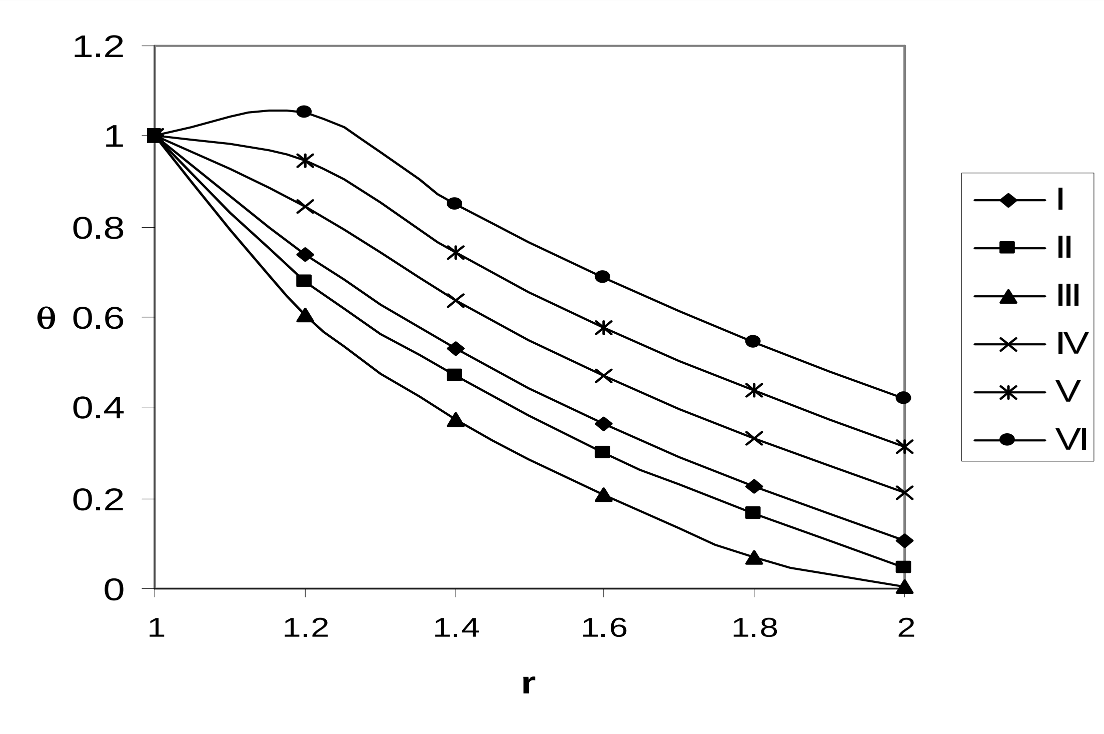

Figure 3(b): Temperature profiles for various values of Kr

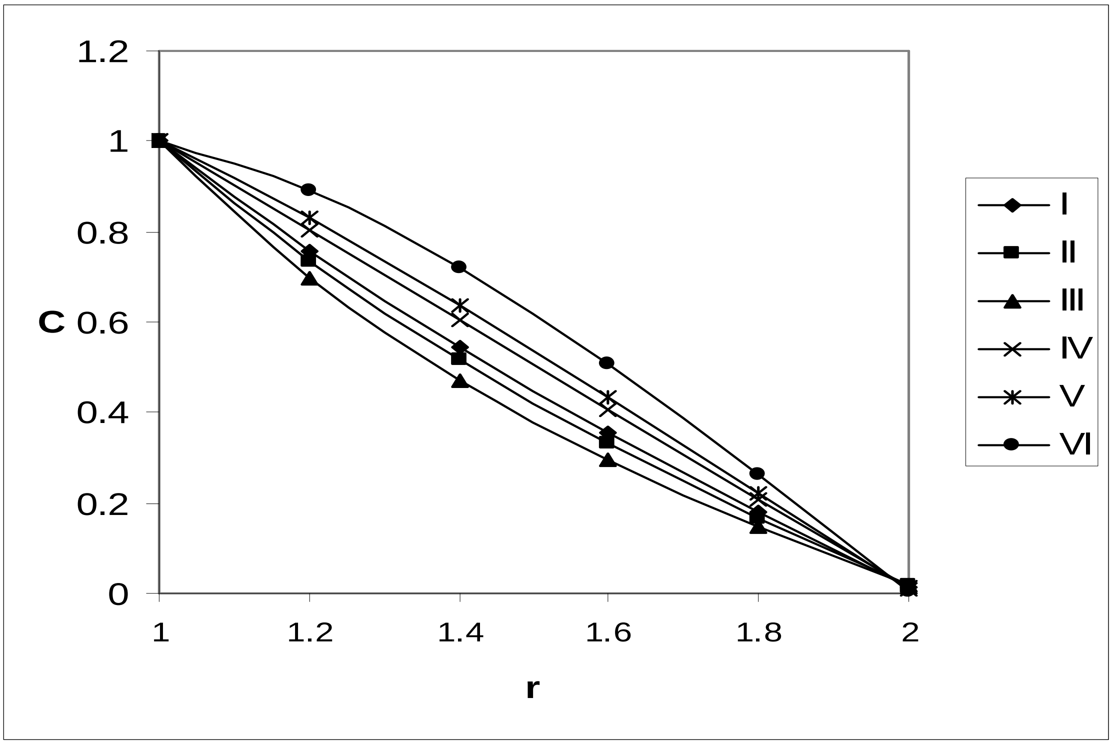

Figure 3(c): Concentration profiles for various values of Kr

Figure 5(a)-5(c) represents the velocity, temperature and concentration distributions for various values of Buoyancy ratio parameter N . **Figures 5(a) and 5(b)** shows that, when the molecular buoyancy force dominates over the thermal buoyancy force. The axial velocity and actual temperature enhances, when the buoyancy forces act in the same direction and for the force acting in the opposite directions, $|w|$ depreciates in the entire flow region. From **figure 5(c),** it is found that the actual concentration reduces with increase of $N > 0$ and enhances with $N < 0$.

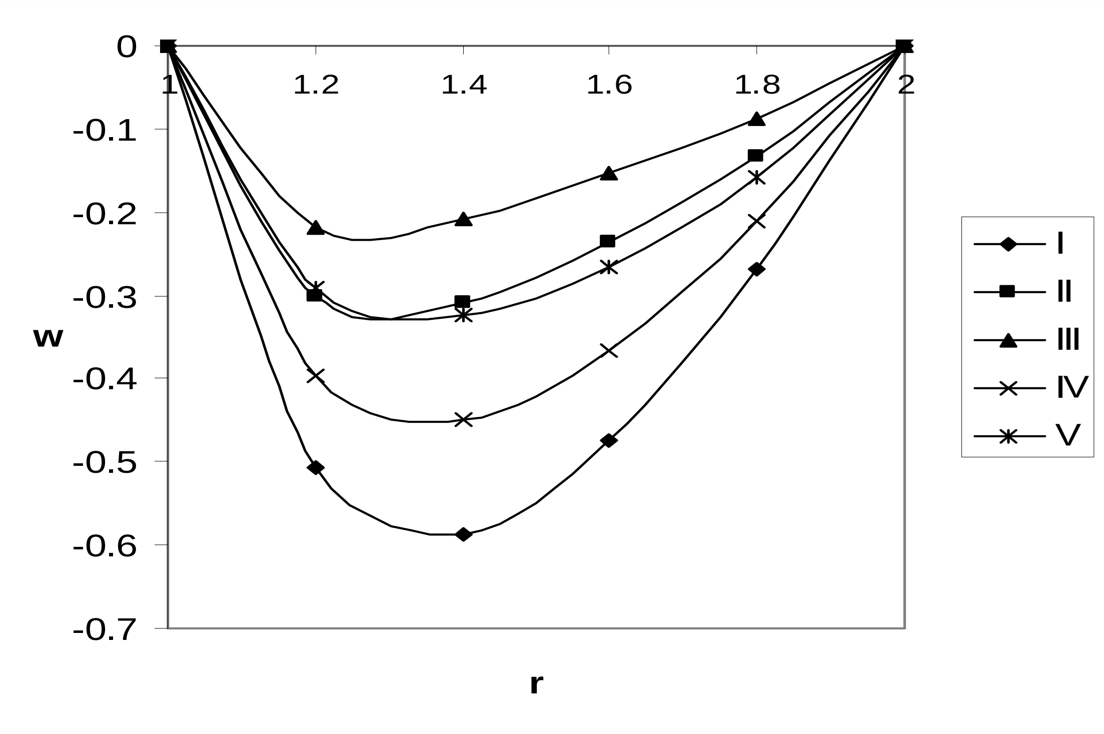

Figure 4 (a): Velocity profiles for various values of D^{-1} and M

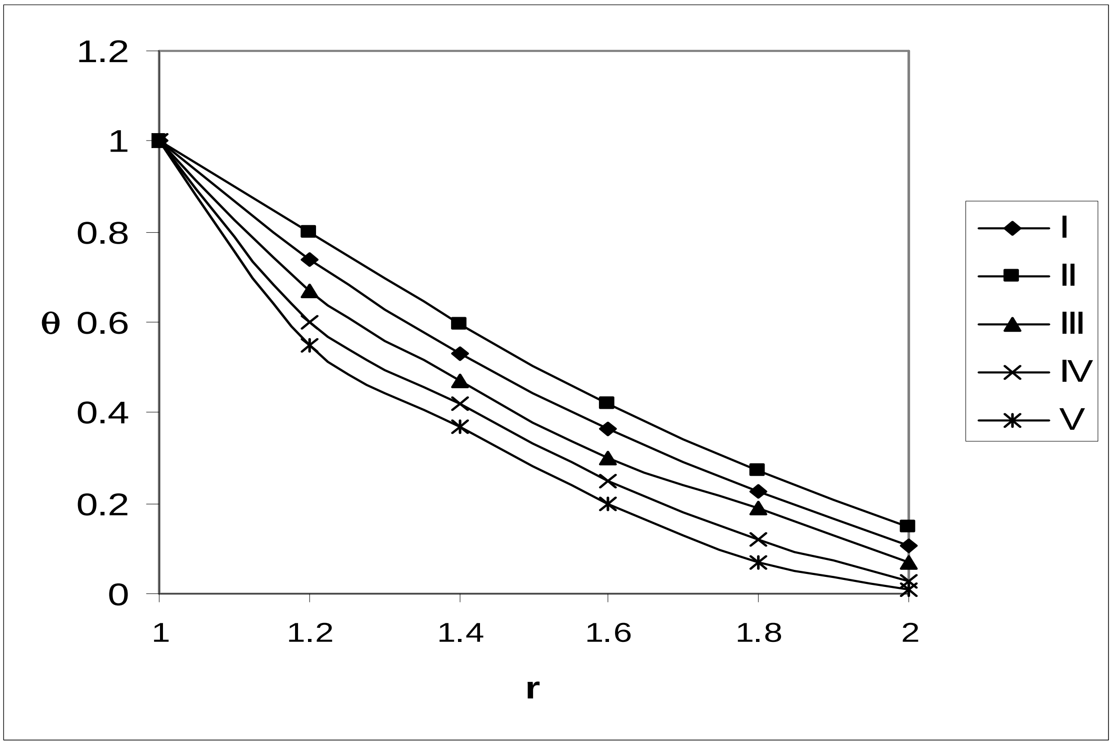

Figure 4 (b): Temperature profiles for various values of D^{-1} and M

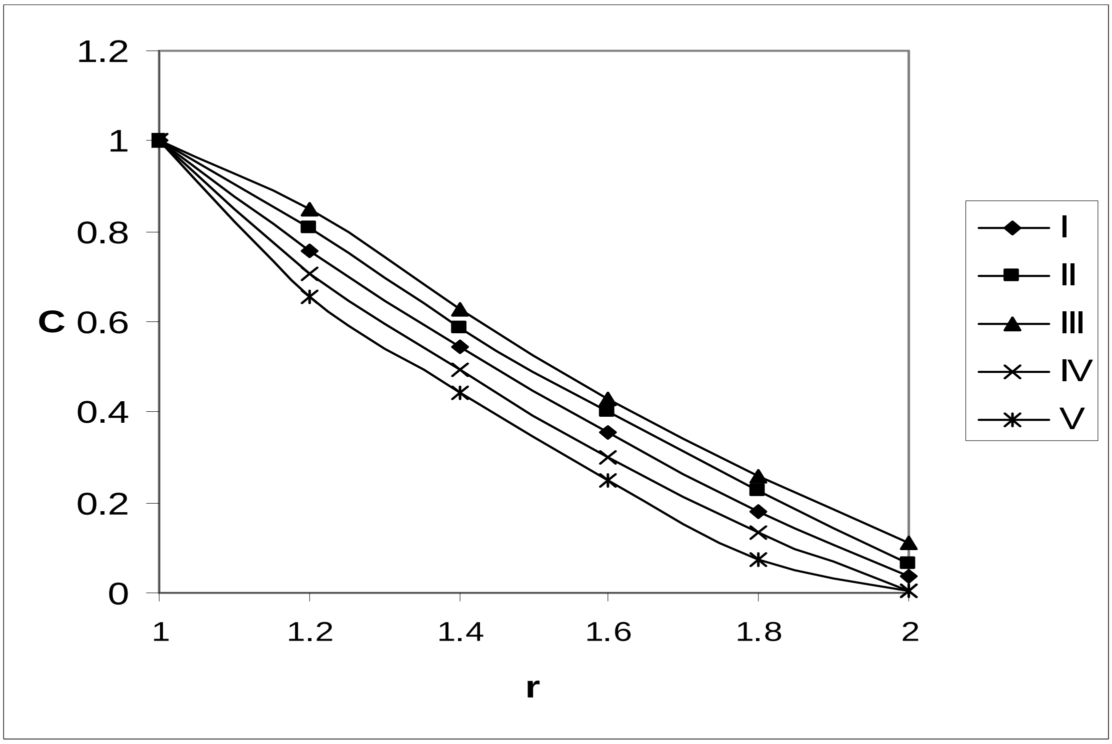

Figure 4 (c): Concentration profiles for various values of D^{-1} and M

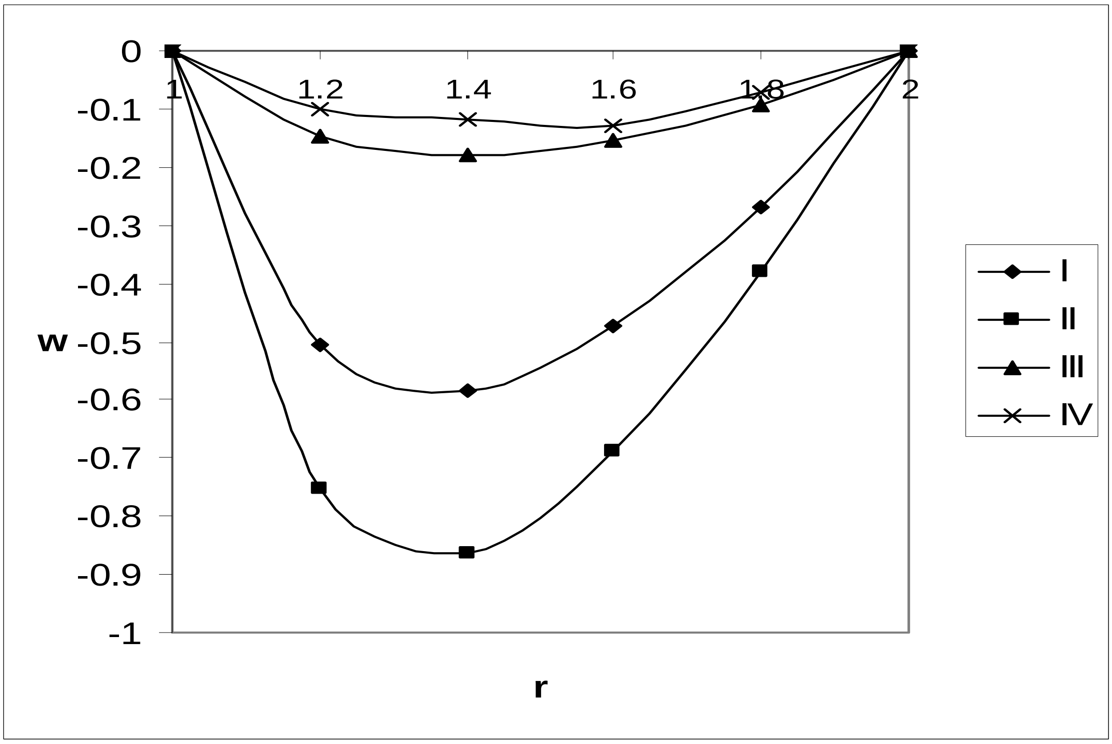

Figure 5(a): Velocity profiles for various values of N

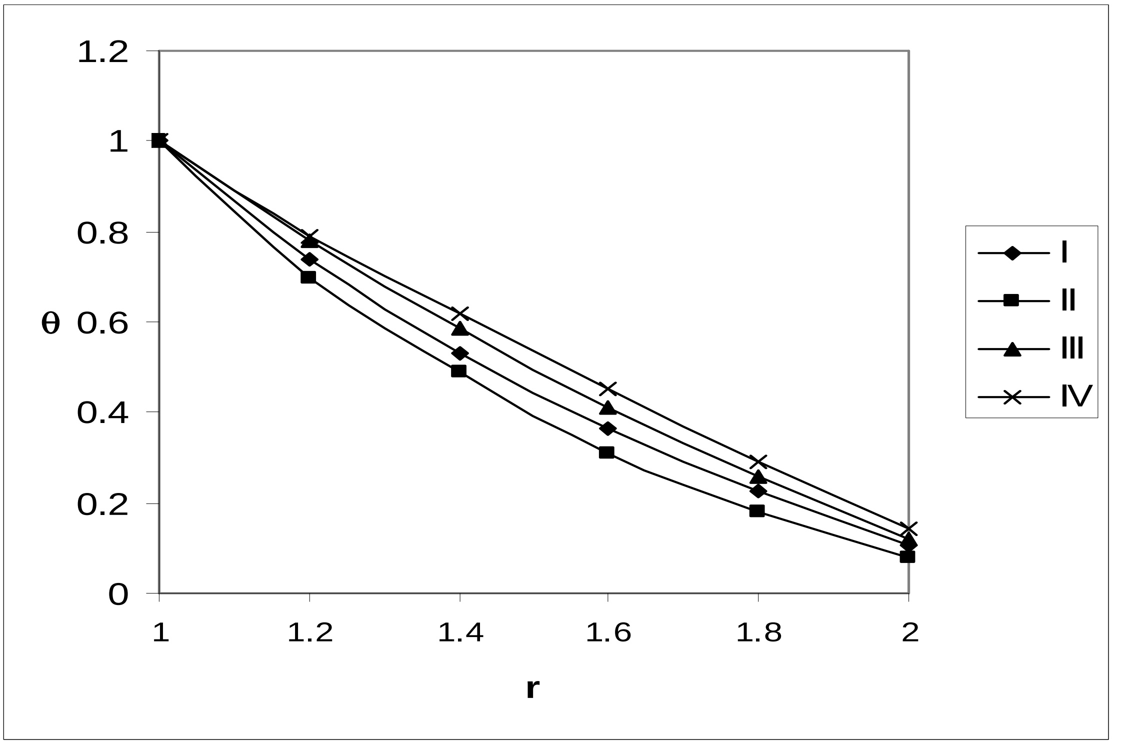

Figure 5(b): Temperature profiles for various values of N

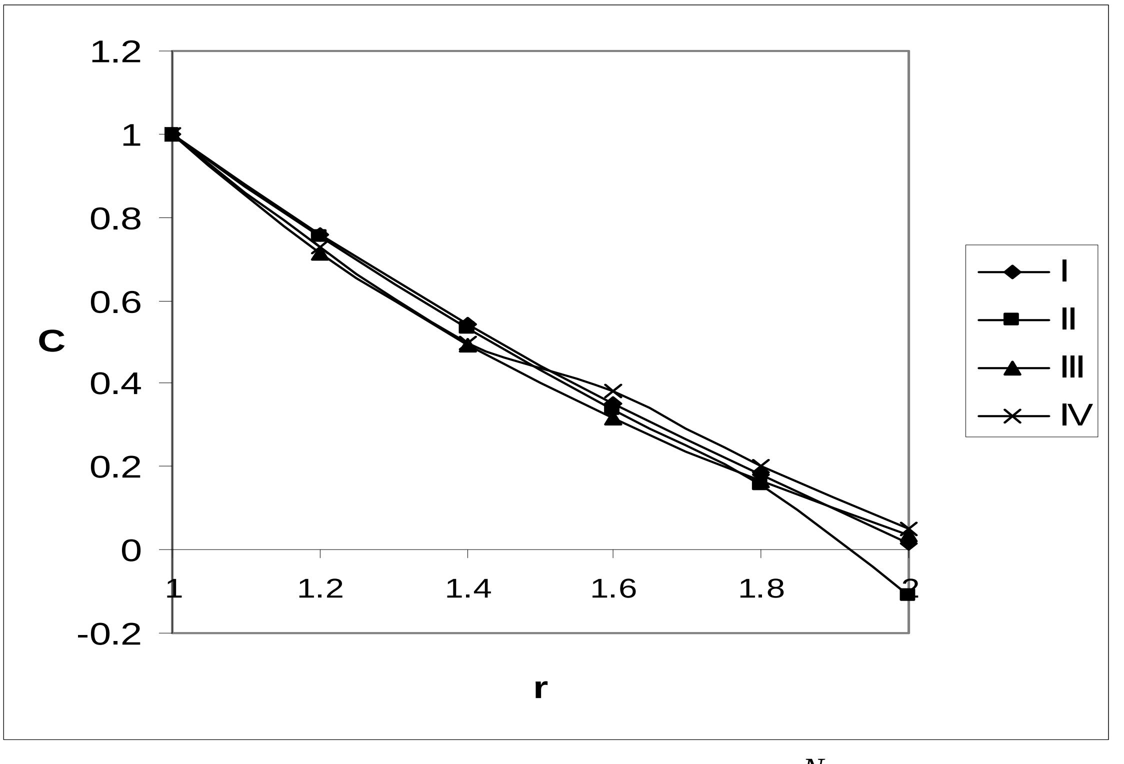

Figure 5(c): Concentration profiles for various values of N

Figure 6(a)-6(c), respectively, show the velocity, temperature and concentration profiles for different values of heat source parameter Q. The variation of $|w|$ with heat source parameter Q shows that $|w|$ depreciates with increase in the strength of the heat generating source (**figure 6(a)**). An increase in the heat source parameter Q enhances the temperature in the entire flow region (**figure 6(b)**). In the degenerating reaction case, the temperature depreciates while it enhances in the generating reaction (**figure 6(c)**). The variation of C with Q shows that the concentration experiences depreciation with increase in Q .

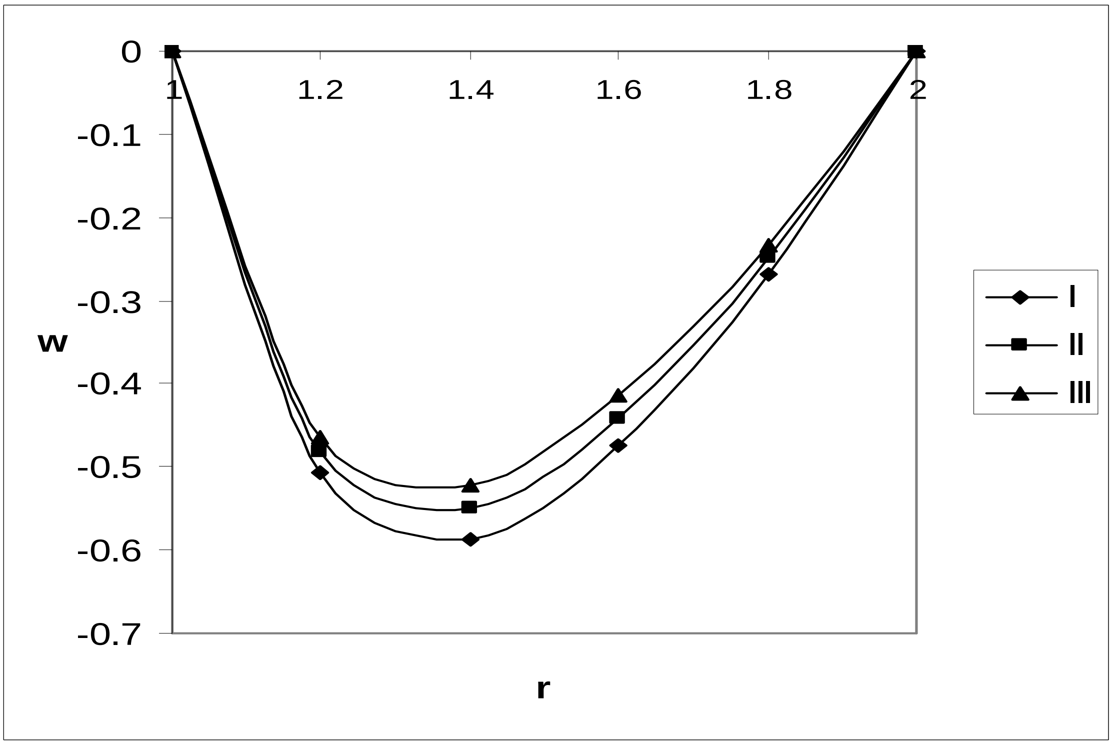

Figure 6(a): Velocity profiles for various values of Q

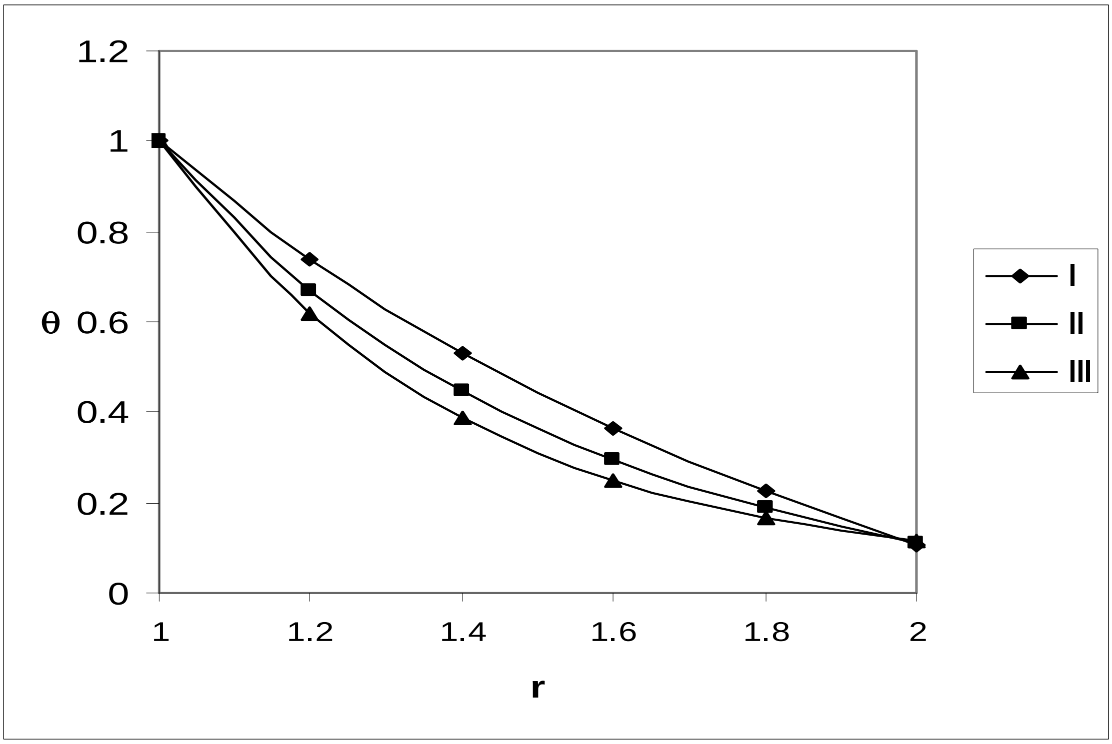

Figure 6(b): Temperature profiles for various values of Q

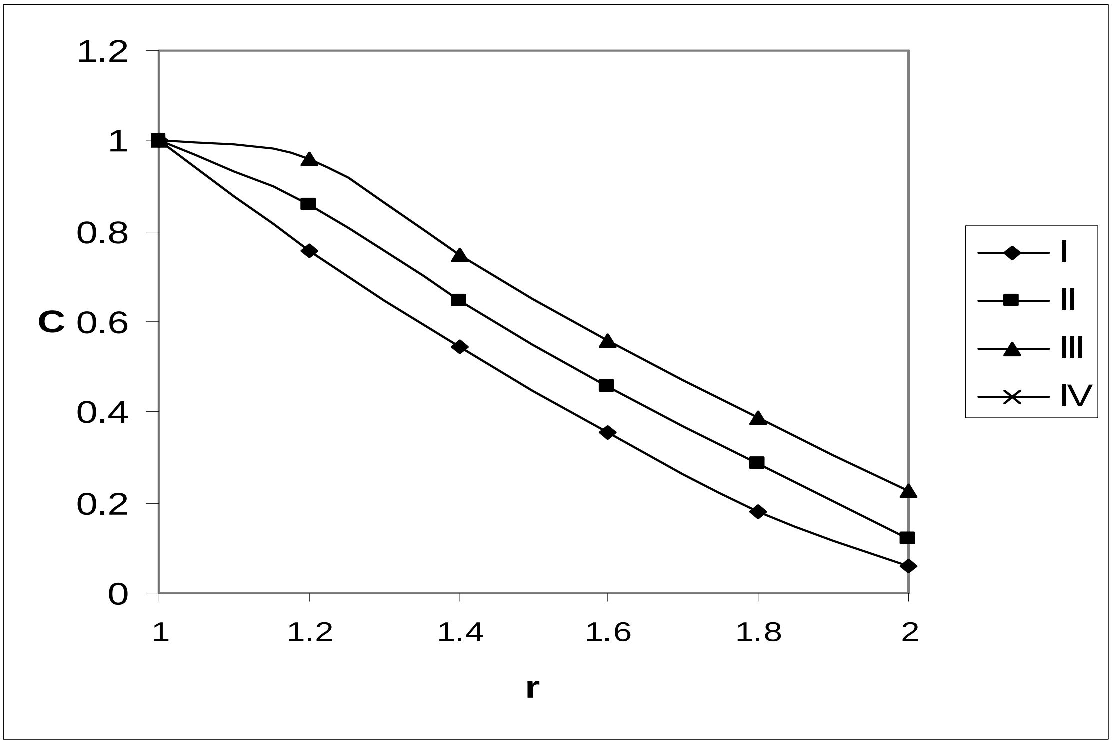

Figure 6(c): Concentration profiles for various values of Q

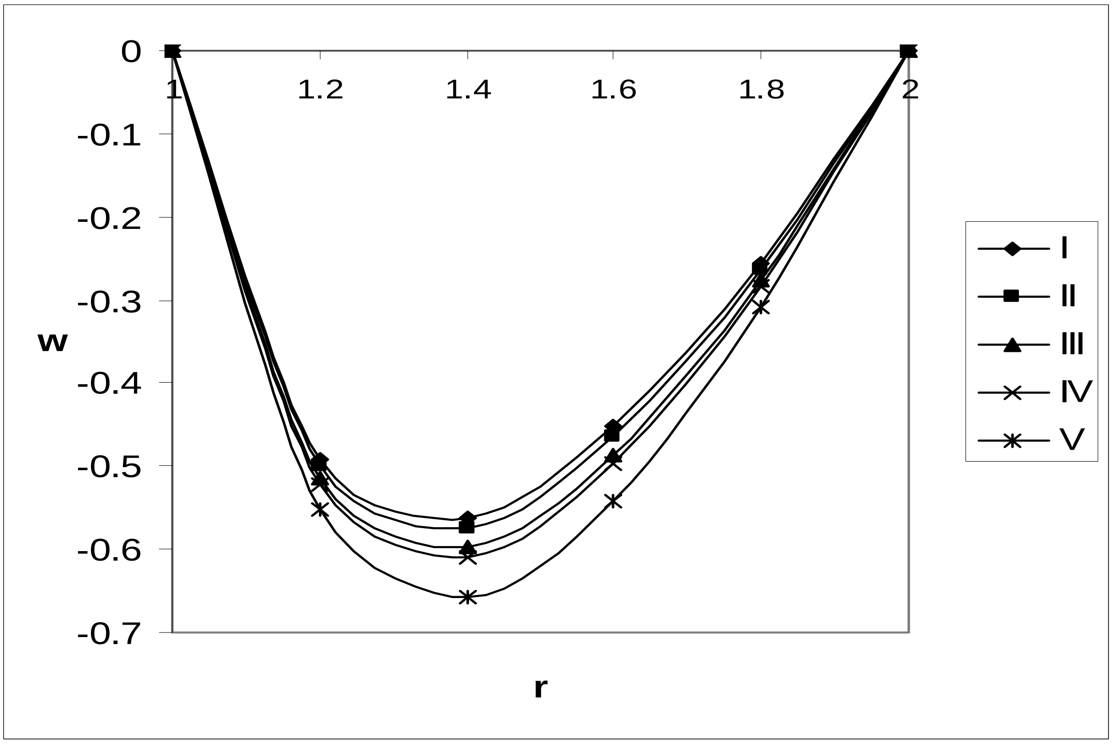

Figure 7(a): Velocity profiles for various values of Q_l

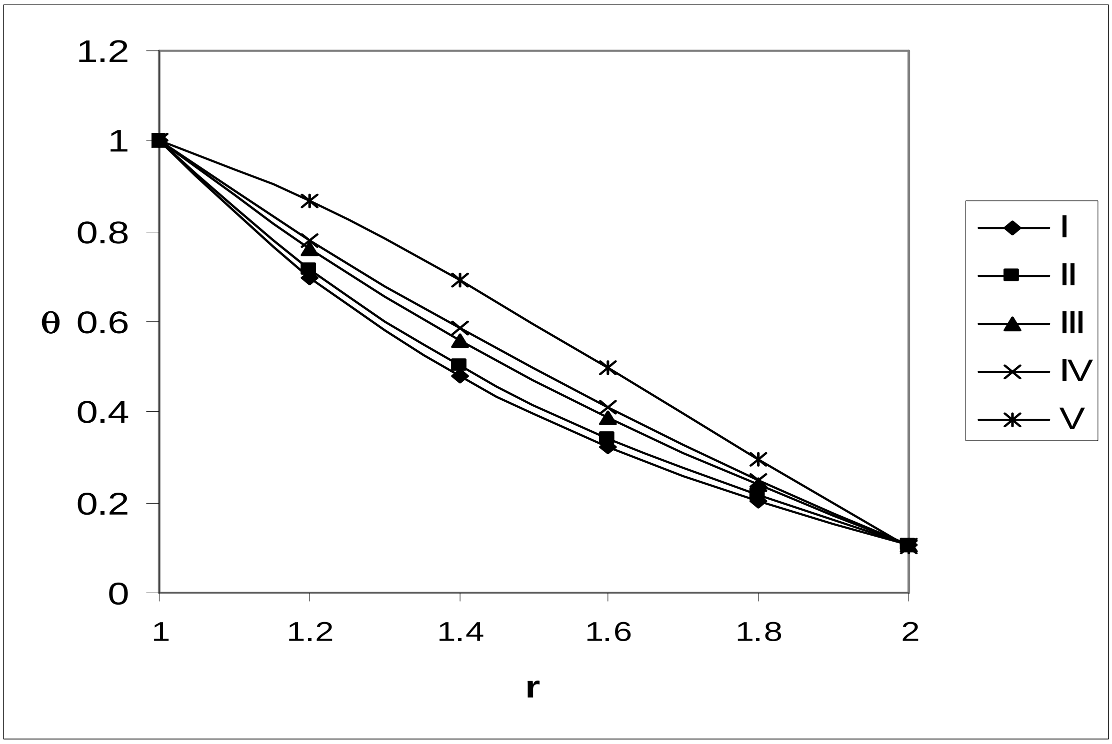

Figure 7(b): Temperature profiles for various values of Q_l

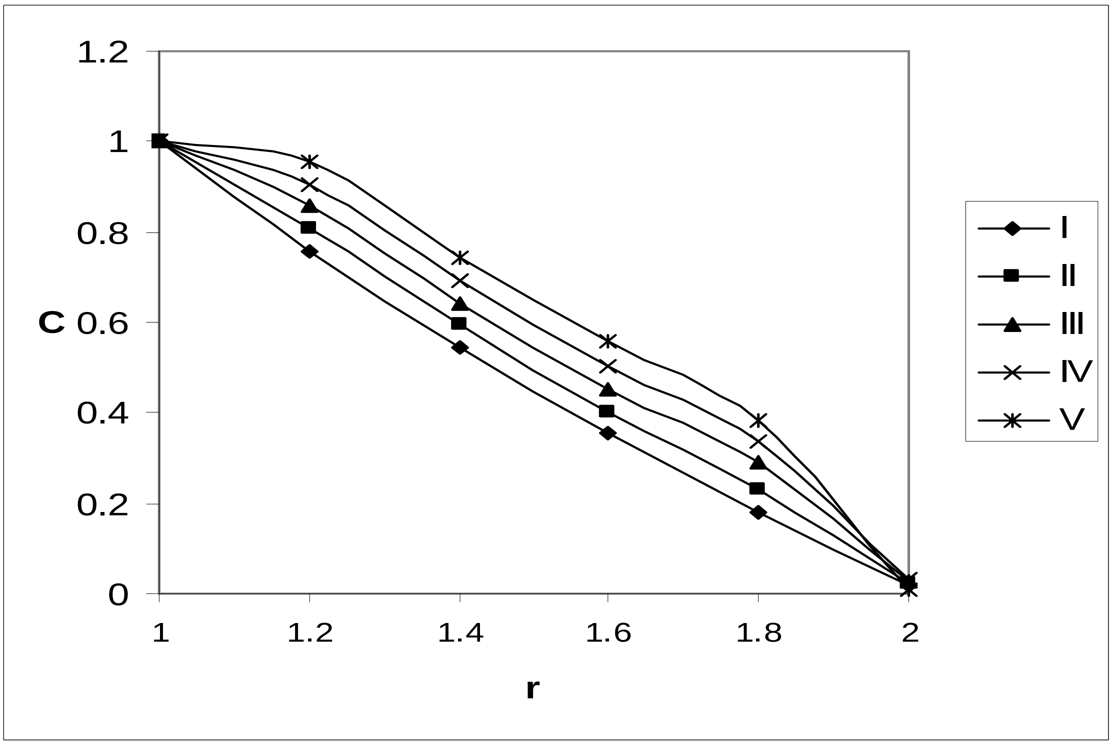

Figure 7(c): Concentration profiles for various values of Q_l

The axial velocity, temperature and concentration distributions are shown in **figures 7(a)-7(c)** for different values of radiation absorption parameter Q_l . The actual axial velocity is in the vertically downward direction i.e. $w < 0$ is the actual flow, and $w > 0$ represents a reversal flow. The variation of $|w|$ enhances with increase in the radiation absorption parameter Q_l (**figure 7**). The variation of θ with radiation absorption parameter Q_l shows an increasing tendency with increase in Q_l everywhere in the flow region (**figure 6**). From **figure 7(c),** it is found that an increase in the radiation absorption parameter Q_l results in depreciation of the concentration in the entire flow region.

Table 1: Shear stress τ at the inner cylinder $r=1$

Gr	I	II	III	IV	V	VI	VII
10	-3.7792	-3.0775	-2.3983	-3.8008	-3.7928	-3.7602	-2.9988
30	-10.0919	-8.3601	-6.8045	-10.757	-10.0929	-10.0748	-8.5673
-10	3.8264	3.12225	2.4296	3.8293	3.8275	3.8243	3.0263
-30	13.4382	11.8445	8.4969	13.1641	13.2818	13.6207	9.8090
D^{-1}	10	10	10	10	10	10	20
Kr	0.5	0.5	0.5	0.5	0.5	0.5	0.5
M	2	4	6	2	2	2	2
N	2	-0.5	-0.8	1	1	1	1
Q	2	2	2	2	2	2	2

Table 2: Shear stress τ at the inner cylinder $r=2$

Gr	I	II	III	IV	V	VI	VII
10	1.4822	1.1836	0.9084	1.3818	1.4356	1.5205	1.0115
30	0.6454	0.0169	0.4037	0.5551	0.6146	0.6452	1.2595
-10	-1.6239	-1.3609	-1.0854	-1.4565	-1.5341	-1.7254	-1.1184
-30	-10.5555	-13.4401	-9.7325	-8.6746	-9.5088	-9.5088	-6.0549
D^{-1}	10	10	10	10	10	10	20
Kr	0.5	0.5	0.5	0.5	0.5	0.5	0.3
R	1	2	-0.5	-0.8	1	1	1
M	2	4	6	2	2	2	2
Q	2	2	2	2	2	2	2

Table 3: Nusselt number Nu at the inner cylinder $r=1$

Gr	I	II	III	IV	V	VI	VII
10	-1.4441	-1.4576	-1.5362	-1.4793	-1.3839	-1.4294	-1.4315
30	-1.8506	-1.9871	-1.9116	-1.8504	-1.7478	-1.6651	-1.61.34
-10	-1.3815	-1.3870	-1.5086	-1.4449	-1.3213	-1.3864	-1.3916
-30	-0.4939	-0.7152	-1.0512	-0.9459	-0.7048	-1.0853	-1.2183
D^{-1}	10	10	10	10	10	20	30
M	4	6	2	2	2	2	2
Q	2	2	2	2	2	2	2

Table 4: Nusselt number Nu at the inner cylinder $r=2$

Gr	I	II	III	IV	V	VI	VII
10	-1.3991	-1.4284	-1.4311	-1.4392	-1.3839	-1.3785	-1.3537
30	-1.4244	-1.4959	-1.5437	-1.4596	-1.4112	-1.4066	-1.3853
-10	-1.3857	-1.3826	-1.4082	-1.4273	-1.3697	-1.3641	-1.3388
-30	-1.3773	-0.8301	-1.4004	-1.4194	-1.3613	-1.3557	-1.3296
Kr	0.3	0.5	1.3	2.3	-0.3	-0.5	-1.3
Q_l	1	1	1	1	1	1	1

Table 5: Sherwood number Sh at the inner cylinder $r=1$

Gr	I	II	III	IV	V	VI	VII
10	-1.2834	-1.2885	-1.2897	-1.4941	-1.3851	-1.1914	-1.2765
30	-1.6825	-1.7048	-1.7265	-1.9294	-1.8021	-1.3734	-1.5146
-10	-1.2369	-1.2243	-1.2176	-1.4632	-1.3486	-1.1294	-1.2324
-30	-0.6511	-0.5557	-0.3665	-0.9501	-0.8043	-0.4957	-0.5829
D^{-1}	10	10	10	10	10	20	30
M	4	6	2	2	2	2	2
Q	2	2	2	2	2	2	2

The Shear stress τ at the inner and outer cylinders $r=1,2$, are evaluated for different parameters are shown in **Tables 1-2**. The stress at $r=1$ enhances with an increase in Gr while at $r=1$, $|\tau|$ depreciates with $Gr>0$ and enhances with $Gr<0$. The variation of τ with M and D^{-1} shows that lesser the permeability of the porous medium higher the Lorentz force, it becomes smaller $|\tau|$ at both the cylinders. An increase in the strength of the chemical reaction Kr and heat source Q leads to a depreciation in the stress at $r = 1, 2$. It is found that when the molecular buoyancy force dominates over the thermal buoyancy force. The stress at $\tau = 1$ enhances irrespective of the directions of the buoyancy forces

Table 6: Sherwood number Sh at the inner cylinder $r = 2$

G	I	II	III	IV	V	VI	VII
10	-1.1983	-1.2834	-1.4814	-1.7313	-1.0085	-0.9416	-0.6502
30	-1.2259	-1.4835	-1.5032	-1.7489	-1.0412	-0.9756	-0.6932
-10	-1.1841	-1.2369	-1.4696	-1.7218	-0.9929	-0.9250	-0.6309
-30	-1.1764	-1.1911	-1.4632	-1.7164	-0.9834	-0.9158	-0.6194
Kr	0.3	0.5	1.3	2.3	-0.3	-0.5	-1.3
Q	1	1	1	1	1	1	1

The Nusselt number Nu at $r = 1$ are shown in **Tables 3-4**. The rate of heat transfer at the inner cylinder enhances with $Gr > 0$ and depreciates with $Gr < 0$. Lesser the permeability of the porous medium or higher the Lorentz force, larger the rate of heat transfer occurs at $r = 1$. An increase in the suction parameter S depreciates Nu for all Gr. The variation of Nu with chemical reaction parameter Kr shows an increase in $Kr \le 0.5$. It enhances the Nusselt number Nu for $Gr > 0$ and depreciates it for $Gr < 0$ and for higher $Kr \ge 0.3$. Also it depreciates with an increase in the radiation absorption parameter Q_l.

The rate of mass transfer at the inner cylinder $r = 1$ which gets enhanced in the heating case and depreciates in the cooling case as shown in **Tables 5-6**. For $Gr > 0$, the rate of mass transfer reduces and enhances for $Gr < 0$, when the buoyancy forces act in the same direction and for the forces acting in opposite direction. An increase in the heat source parameter Q, chemical reaction parameter Kr and M or D^{-1} reveals that the rate of mass transfer reduces in heating case and enhances in the cooling case. With respect to the chemical reaction parameter Kr, it is found that the rate of mass transfer experiences an enhancement in the decreasing chemical reaction and depreciates in the generating reaction. Further, it enhances with an increase in the radiation absorption parameters Q_l.

NOMENCLATURE

C	concentration
C_e	concentration in the equilibrium state
C_P	specific heat at constant pressure
D_1	molecular diffusivity
D_2^{-1}	Darcy parameter
Gr	Grashof number
k	porous permeability
k_f	coefficient of thermal conductivity
kl	chemical reaction coefficient
Kr	chemical reaction parameter
M	Hartmann number
N	Buoyancy ratio parameter
P_e	pressure
P_d	dynamic pressure
$\Pr$	Prandtl number

GREEKWORDS

$\beta^\bullet$	volumetric expansion with mass fraction
ρ	density of the fluid
μ	coefficient of viscosity
μ_e	magnetic permeability
σ	electrical conductivity
ρ_e	density
Q	Heat Source parameter
Q	heat generating source
Q_1	radiation absorption parameter
S	suction parameter
Sc	Schmidt number
T	temperature
T_e	temperature in the equilibrium state
(u, w)	velocity components

REFERENCES

[1] V. Prasad, Natural convection porous media. *Ph.D thesis*, Sri Krishnadevaraya University, Anantapur, (**1983**) India.
[2] P.M.V. Prasad, Hydromagnetic convection heat and mass transfer though a porous medium in channels / pipes. *Ph.D thesis*, S.K.University, Anantapur, (**2006**) India.
[3] Prasad and F.A. Kulacki, *International Journal of Heat and Mass transfer,* 27(**1984**) 207.
[4] Y.F. Rao, Y. Miki, Y. Fulluda takata and S. Hasegahea. *International Journal of Heat and Mass transfer*, 28 (**1985**) 705.
[5] Miheersen and K.E. Torrance. *International Journal of Heat and Mass transfer*, 30(4) (**1987**) 729.
[6] N. Faces and B. Faroup. *ASME, Journal of Heat transfer*, 105 (**1982**) 680.
[7] M.A. Harstad and P.J. Burus. *International Journal of Heat and Mass transfer,* 25(1) (**1982**) 1755.
[8] L. Robillard, T.H. Nguyen, M.G. Satish and P. Vassueur, Heat transfer in porous media and particulate flows. *Ame. Soc. Mech. Engg, Htd*, 46 (**1985**) 412, New York.
[9] P. Vasseeur, T.H. Ngugen, L. Robillard and V.K.T. Thi. *International Journal of Heat and Mass transfer,* 27(**1984**) 337.
[10] Miheersen and K.E. Torrance. *International Journal of Heat and Mass transfer*, 30(4) (**1987**) 729.
[11] J.F. Osterle and F.J. Young. *Journal of fluid Mechanics*, 11(**1961**) 152.
[12] G. Roots. *International Journal of Heat and Mass transfer* l3 (**1961**)1.
[13] K.R. Singh and T.J. Cowling. *Q. Journal of Maths Appl. Maths*, 16 (**1963**)1.
[14] C.P. Yu, *Appl Sci. Res*, 22 (**1970**) 127.
[15] C.P. Yu and H. Young. *Appl Sci. Res*, 20 (**1969**) 16.
[16] V.U.K. Sastri and C.V.V. Bhadram. *App. Sci. Res*, 34(2/3) (**1978**) 117.
[17] R.S. Nanda and R. Purushottam. *Int. Dedication seminar on recent advances on maths and application,* (**1976**) Varanasi.
[18] R. Ganapathy and R. Purushothama, Fluid flow induced by a travelling (**1990**).
[19] J.A. Whitehead, *Geo Phys. Fluid dynamics*, 3 (**1972**) 161-180.
[20] T.S. Chen and C.F. Yuh, *Journal of Heat transfer*, 2 (**1979**) 233-350.
[21] P.V. Satya Narayana and B. Venkateswarlu, *Journal of Heat Transfer Asian Research* (**2013**) DIO.10.htj.21101.
[22] P.V. Satya Narayana and B. Venkateswarlu and S. Venkataramana, *Ain Shams Engineering Journal*, 4(4) (**2013**) 843-854.
[23] P. Sivanjaneya Prasad, Effects of convective heat and Mass transfers on unsteady hydromagnetic channel flows. *Ph.D thesis,* S.K. University, Anantapur, (**2001**) India.
[24] Antonio Barletle *International Journal of Heat and mass transfer*, 42 (**1999**) 2243-2253.
[25] Shaarwari.ElM.A.I and A. Nimr. M.A, *International Journal of Heat and mass transfer*, (**1990**) 1873-1884.
[26] M.A. Al-Nimr, *International Journal of Heat and mass transfer*, 36 (**1993**) 2388-2395.
[27] J.R. Philip, *International Journal of Heat and mass transfer,* 25 (**1982**) 1689-1699.
[28] B. Venkateswarlu and P.S. Satya Narayana, *Applied Nanoscience* (**2014**).
[29] P.V. Satya Narayana, B. Venkateswarlu and S. Venkataramana, *Journal of Energy Heat and Mass Transfer* 35 (**2013**)197-214.
[30] P.V. Satya Narayana, B. Venkateswarlu and S. Venkataramana, *Walailak Journal of Science and Technology* (**2014**).